Long duration (>4 Ma) and steady-state volcanic activity in the early Cretaceous Paraná–Etendeka Large Igneous Province: New palaeomagnetic data from Namibia

Sarah C. Dodd [a,*], Conall Mac Niocaill [b], Adrian R. Muxworthy [a]

[a] *Dept. of Earth Science and Engineering, Imperial College London, South Kensington, SW7 2AZ, UK*
[b] *Department of Earth Sciences, University of Oxford, South Parks Road, OX1 3AN, UK*

ARTICLE INFO

ABSTRACT

There is long-standing correlation between Large Igneous Provinces (LIPs) and major mass extinction events in the Geological Record, postulated to be due to the emission of large quantities of volcanic gases over a geologically short period of time causing major climatic perturbations within the Earth system. The ∼135 Ma Paraná–Etendeka volcanic province of Brazil and Namibia represents something of an enigma amongst LIPs. Despite an erupted volume (>1 Mkm^3) comparable to other LIPs associated with mass extinctions, such as the Siberian or Deccan traps, it is not linked to a known mass extinction event. This suggests that the Paraná–Etendeka volcanic province was emplaced over longer timescales than other LIPs, and/or emitted a lower concentration of volatiles, directly or indirectly during its emplacement.

We present a new, detailed magnetostratigraphy for the Etendeka portion of the province that suggests emplacement took place over longer timescales (>4 Ma) than those associated with other LIPs. Palaeomagnetic analysis of 893 specimens from 99 sites, in sections that encompass nearly the complete Etendeka stratigraphy, yielded high-quality data from 70 sites (612 specimens). These record 16 individual polarity intervals, which can be correlated with Chrons 15 to 11 of the geomagnetic polarity time scale (GPTS) while also providing two new, high quality palaeopoles for South Africa at 130–135 Ma. Our magnetostratigraphy reveals a minimum period of volcanic activity in excess of 4 Myrs and, importantly, we find no evidence for major changes in the rates of volcanic activity through that time period, in contrast to other LIPs where volcanism seems to be concentrated in major pulses. This suggests that the anomalously feeble environmental impact of Paraná–Etendeka volcanism may be due to lower effusion rates reducing the atmospheric loading due to volcanogenic volatiles.

1. Introduction

Large igneous provinces (LIPs) are magmatic regions covering sizeable areas (typically >0.1 Mkm^2) comprising large volumes of extruded igneous material (many LIPs >1 Mkm^3) emplaced over geologically short periods of time (1–5 Ma) (e.g. Bryan and Ferrari, 2013; Coffin and Eldholm, 1994; Courtillot, 1994). Some, but not all, LIPs have been linked to episodes of major climatic changes in the geological past, including mass extinctions of biota (Wignall, 2001). For example, the eruption of the Siberian LIP at the Permo-Triassic boundary, the Central Atlantic magmatic province (CAMP) at the Triassic–Jurassic boundary, and the Deccan Traps at the Cretaceous–Palaeogene boundary have been linked with mass extinctions, major changes to the climate system, and major changes in the carbon cycle (e.g. Black et al., 2012; Blackburn et al., 2013; Courtillot et al., 2000). In order to understand the role these provinces may have played in major climatic and environmental changes we ideally need to know the duration of volcanism, their tempo, and the volatile flux of each province. Constraints on these parameters are hard to obtain, although rapid progress is being made in several of these areas (e.g. Blackburn et al., 2013; Chenet et al., 2008; Courtillot and Fluteau, 2014; Jay and Widdowson, 2008; Self et al., 2014). Notwithstanding this, a key question emerges: why do some LIPs appear to have been associated with major environmental changes and mass extinctions, whereas others of similar size and apparent duration appear to have had only limited environmental impact?

One such enigmatic LIP is the lower Cretaceous (≈135 Ma) Paraná–Etendeka province, now exposed in South America and Africa, with a total volume estimated to exceed 1 Mkm^3 and

---

* Corresponding author.
E-mail address: sarah.dodd@worc.oxon.org (S.C. Dodd).

an area greater than 1.2 Mkm^2 (Peate, 1997). Despite its large area and volume (approximately equivalent to the Siberian traps (1–2 Mkm^3)), the province appears to have had little environmental impact (Wignall, 2005) and the duration of volcanism remains uncertain (Courtillot and Renne, 2003).

The Paraná–Etendeka province has been extensively studied for both geochronology and paleomagnetism, including both the extrusive (e.g. Ernesto and Pacca, 1988; Ernesto et al., 1999; Renne et al., 1996b) and intrusive (e.g. Raposo et al., 1998; Renne et al., 1996a) portions of the now-rifted province. Several of these studies attempt to establish a range of absolute ages (e.g. Ernesto et al., 1999; Pinto et al., 2011; Renne et al., 1992), while the paleomagnetic studies generally focus upon the number of reversals recorded within the extruded stratigraphy (e.g. Ernesto and Pacca, 1988; Renne et al., 1992, 1996b). Absolute age based studies, dominated by ^{40}Ar/^{39}Ar chronology, have resulted in a conflicting history of timeframes ranging from 11 Myrs (Turner et al., 1994) to <1 Myr durations (Renne et al., 1996b). Many ^{40}Ar/^{39}Ar estimates were obtained by the laser total fusion method, since found to produce misleading results (Thiede and Vasconcelos, 2010) and subsequently rendering numerous early estimates unreliable. The most recent synthesis by Janasi et al. (2011) supports a ≈3 Myr timeframe for volcanic activity, yet also highlights the small number of reliable estimates (by ^{40}Ar/^{39}Ar step heating or U–Pb) that sample the extrusive stratigraphy (Ernesto et al., 1999; Janasi et al., 2011; Pinto et al., 2011; Renne et al., 1992, 1996b; Thiede and Vasconcelos, 2010) and overlying/intruding units (Wigand et al., 2004).

Existing palaeomagnetic analyses provide a similarly fragmented picture, with Ernesto and Pacca (1988); Ernesto et al. (1990, 1999) and Renne et al. (1992) presenting data from short palaeomagnetic sections from across the Paraná. The interpretation of the resulting magnetostratigraphy is varied. Renne et al. (1992) suggest short timescales of emplacement of the Paraná portion of the province given the infrequency of reversals (no single section recorded more than four reversals), whereas Milner et al. (1995) suggest that, considering the relative stratigraphic position of the multiple sections in Ernesto and Pacca (1988), a minimum of ten polarity intervals were identifiable. With no continuous section through the volcanic stratigraphy and only partial sections requiring correlation, different interpretations can lead to contrasting estimates of duration depending whether individual sections are correlated or stacked. To date, only one paleomagnetic study of the Etendeka has been published; that of Renne et al. (1996b), presented also in Marsh et al. (2001) and Marsh and Milner (2007). The Renne et al. (1996b) study was argued to provide evidence for a short duration (0.6 ± 1.0 Ma) emplacement for the Etendeka portion of the province by virtue of the fact that their study only yielded one reverse chron per stratigraphic section sampled.

Despite many studies it is clear, following the recent synthesis of Janasi et al. (2011) which constrained activity to ≈3 Myrs, that the available ages are, as yet, insufficient to provide a detailed province history. It is also apparent that, although numerous magnetostratigraphic studies have concentrated on the Paraná portion of the province, limited magnetostratigraphy is available for the Etendeka portion, where larger portions of stratigraphy can be sampled at a single location and where correlation between fewer, detailed and longer sections may be more easily established. We thus report a new detailed magnetostratigraphic investigation of the Etendeka portion of the province to better constrain the timescales of volcanism in the Paraná–Etendeka LIP.

2. Regional geology and sampling

2.1. The Etendeka geology

The term 'Etendeka traps' is normally used to refer to the extrusive and intrusive volcanic rocks that lie between the latitudes 22° S and 17°10′ S in Namibia (Fig. 1). The extrusive rocks studied are bimodal in composition but the majority of the extrusive sequence is composed of three mafic flow types; the Tafelberg, Tafelkop and Khumib basalts. In the area sampled, the Tafelberg (upper) and Tafelkop (lower) basalts dominate the mafic stratigraphy (Miller et al., 2008). Punctuating this dominantly mafic stratigraphy are a number of silicic rheoignimbrite sheets, known collectively as the Etendeka Quartz Latites (QL)s (>65% SiO$_2$) and Latites (<65% SiO$_2$) (Erlank et al., 1984), and these are used as stratigraphic marker beds (Milner et al., 1992).

Sitting above the central (Springbok) QL, is a large-scale erosional surface known as the intra-Etendeka unconformity or disconformity II (Jerram et al., 1999; Miller et al., 2008; Milner et al., 1994). Because of this, all sampled sections have been split into those falling above ('Etaka' subgroup) and those below ('Awahab' subgroup) this surface (Miller et al., 2008). Partially conflicting views exist regarding the stratigraphic relationship of the upper and lower portions of the Etendeka and the unconformity, with Marsh and Milner (2007) suggesting the Awahab and Etaka were actually emplaced coincidentally rather than representing young and old counterparts. If true, this should allow the recorded magnetostratigraphy of the Awahab and Etaka subgroups to be correlated rather than stacked between sections. Part of the evidence for correlating the Awahab and Etaka subgroups was the then-available magnetostratigraphy for the Tafelberg and Awahab (Renne et al., 1996b). We will show later, on the basis of our new results, that this correlation is unlikely.

The Etendeka is also commonly geographically divided, based on both compositional and structural characteristics: (1) compositionally, the province is split into northern and southern sections the north characterised by high-Ti contents (>2.2%) and south of 19°21.6′ S characterised by low-Ti contents (<2.2%) (Ewart et al., 1998; Marsh et al., 2001); and (2) structurally, the province is split into inland and coastal sections (Marsh et al., 2001). Inland sections are characterised by the signature horizontally bedded volcanic successions common within LIPs; however, some minor faulting occurs towards the coastal sections that are characterised by complex listric faults (Marsh et al., 2001). Due to the intrinsic problems with correlating the heavily faulted sections in the absence of geochemical data, the complex coastal areas were avoided, meaning that all of the sampled sections in this study lie within the inland structural section. In the northern (high-Ti) domain the mafic stratigraphy is dominated by the Khumib basalts. These basalts are accompanied by a series of interfingering QLs and minor basaltic units largely confined to these northern or coastal regions (Miller et al., 2008). The Khumib sequence has a poorly understood interfingering relationship with the lower Tafelberg basalts of the southern domain that hampers detailed correlation between these two domains. We confined our sampling to the better understood, southern domain (Fig. 1).

2.2. Sampling methods and localities

Samples were collected from three continuous stratigraphic sections containing no identifiable sills (herein referred to as the Grootberg, Messum and Tafelkop sections) in addition to two short sections (referred to as the Bergsig and Fonteine mini-sections) and a number of individual sampling sites. Samples were predominantly collected as drill cores, yielding a total of 737 cores from 81 sites. Due to mechanical problems with our rock drill during two
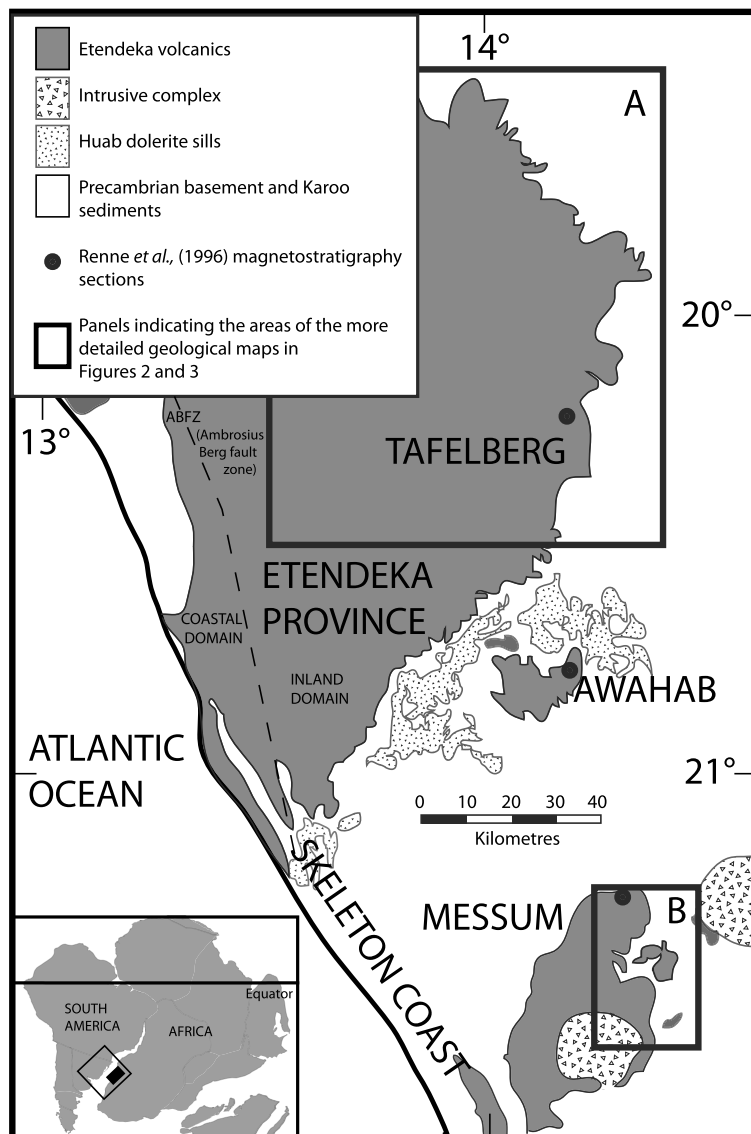
Fig. 1. A simplified geological map of the sampled regions of the Etendeka province modified from Renne et al. (1996a, 1996b). The panels labelled A and B show the broad localities of the sampled sites and the area of the more detailed site maps of Fig. 2 (A and B). The localities of the previous (Renne et al., 1996a, 1996b) magnetostratigraphic sections are also indicated. The small inset map shows the location of the map region (shaded rectangle) within the larger Paraná–Etendeka province (larger rectangle) in a 135 Ma pre-drift reconstruction.

field seasons, oriented hand-samples were collected at a further 18 sites, yielding 149 individually oriented hand-samples. Samples were oriented using both magnetic and sun compasses where possible and an accompanying clinometer. Comparison of the magnetic and sun compass measurements revealed that bearings were generally within 5° supporting the integrity of the magnetic measurements. For sites where the bearings differed by >5°, sun compass values were used. The locations and sites sampled in these sections are illustrated in Fig. 2 and further described below.

2.2.1. The Etaka subgroup

The Grootberg section and the Bergsig mini-section sample the stratigraphy above the intra-Etendeka unconformity. The Grootberg section, runs through the Grootberg pass from 19°50′34″ S, 14°07′44.46″ E to 19°52′25.34″ S, 14°03′50.65″ E (Fig. 2a), and samples nearly the complete 'Etaka' subgroup. A high sampling density was possible due to almost continuous exposure resulting in an excellent vertical section through this uppermost portion of the Etendeka stratigraphy. The Bergsig mini-section samples up rivers that incise the north facing slope of the local topographic

high centred on 20°10′53.92″ S, 14°04′32.43″ E (Fig. 2a). The section samples portions of the Wêreldsend QL and the basaltic units directly below, which can be correlated with the Grootberg section lying approximately 40 km away due north. In this northern region all of the volcanic units sampled are approximately horizontal with sub-degree dips towards the south generating the small 90 m altitude difference between the Wêreldsend QL exposed in the Grootberg and Bergsig sections.

2.2.2. The Awahab subgroup

The Messum and Tafelkop sections, the Fonteine mini-section, and all individual sites sample the stratigraphy beneath the intra-Etendeka unconformity (Fig. 2). The Messum section samples the units directly below the unconformity. In this southern region the volcanic rocks are dipping measurably in a radial sense towards the Messum crater, an artefact postulated to be the result of downsag following the voluminous Goboboseb and Springbok QL eruptions sourced from the Messum crater, with estimated volumes of 2300 km^3 and ≤6300 km^3 respectively (Ewart et al., 2002; Milner et al., 1995). The section samples a laterally extensive area
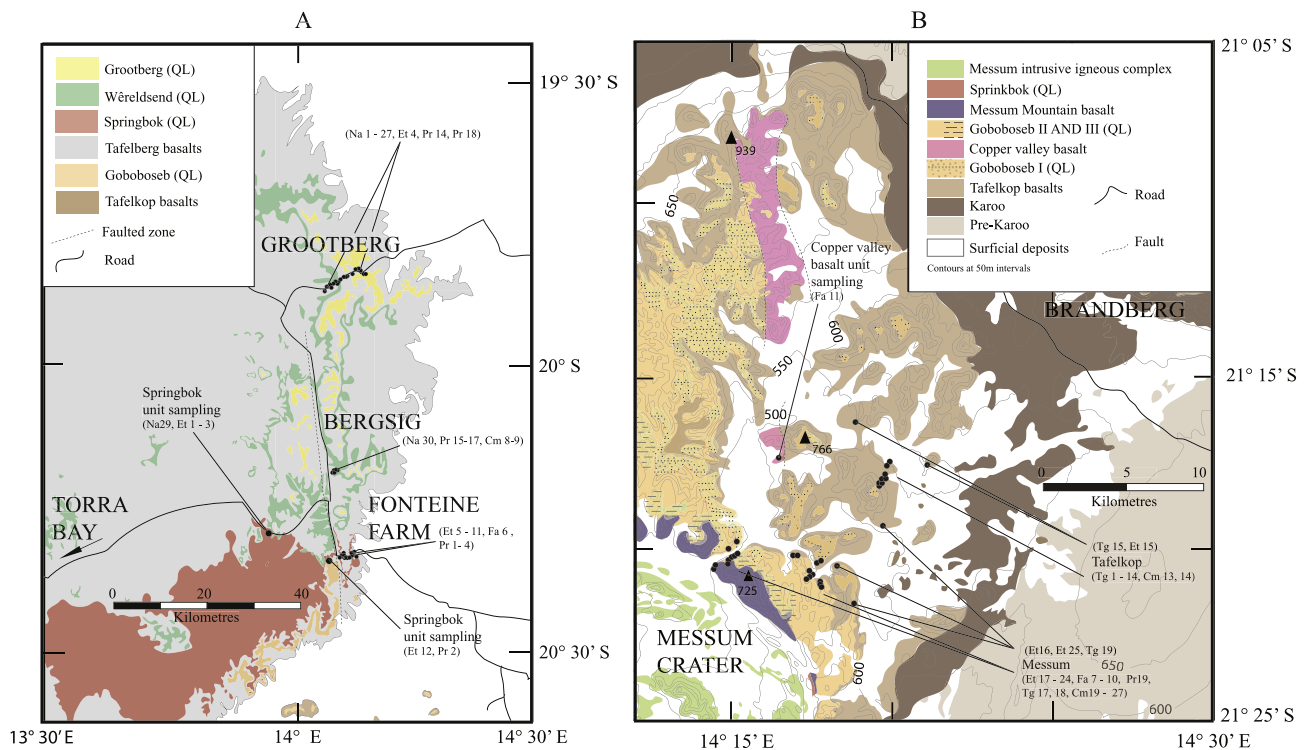
Fig. 2. Detailed geological maps of the Northern pane (A) and Southern pane (B) indicated in Fig. 1. Panel A shows the localised geology and sampled sections and sites in this Northern region. The map has been modified from the maps of Milner et al. (1992) and Miller et al. (2008). Panel B shows the localised geology and sampled sections in the southern Messum region. The geology is based on that published in Miller et al. (2008) and a simplified topography has been overlain. The south–west corner of this map is taken to be the approximate centre of the Messum crater in later calculations.

that can be split into two individual tracks following the rough incision paths of tributaries of the Messum river (Fig. 2b). One track follows an approximately linear trend beginning at the Messum crater edge at 21°20′40″ S, 14°14′20.30″ E and ending at 21°19′43.63″ S, 14°15′09.86″ E, and the other follows a circumference like path (taking 21°25′0″ S, 14°12′55″ E as the crater centre) from 21°19′59.67″ S, 14°16′42.63″ E to 21°20′45.10″ S, 14°17′46.36″ E (Fig. 2b) with the relative position of sites well established through observed relationships in the field. Three sites, (Et16, Et25 and Tg19) lie further to the east, off these main paths (Fig. 2b).

The Tafelkop section samples the oldest sequence of basalts in the southern domain: the Tafelkop basalts. It samples from the lowest flows upwards towards the units sampled in the Messum section. The majority of sites featuring in the Tafelkop section sample up small river valleys incising the north west slope of a local topographic high running from the highest site, Tg5 at 21°18′12.06″ S, 14°19′21.00″ E, to the lowest site Tg1A/B at 21°17′25.02″ S, 14°19′39.60″ E (Fig. 2b). Two further sites feature in this section, Et15 and Tg15 (Fig. 2b). These sites lie within 1 km of the main section sampled, with their relative position at the base of the sampled stratigraphy well established. The lateral separation from the main Tafelkop sequence, however, means that their vertical position relative to other sites was estimated by projecting them onto the main line of section using their relative radial distances and bed dips. As the radial distance to the Messum crater increases, the dip on the beds decreases, such that in the region of the Tafelkop section the beds are dipping an average of only 5° as opposed to in the Messum region where the average dip is ~11°.

The Fonteine mini-section samples along a road section from 20°19′52.80″ S, 14°05′31.14″ E to 20°19′19.03″ S, 14°07′15.56″ E (Fig. 2a). It samples just below the unconformity with the strati-

graphically highest unit sampled being the Springbok QL that is partially eroded by the surface of the unconformity.

The Springbok QL is sampled by four sites (Na29, Et1, Et2 and Et3) in roadside outcrops approaching Torra Bay, and by another site (Pr2) located on a track towards the Damaraland camp (Fig. 2a). The site Et12, also along the Damaraland camp track, samples the basaltic unit found below this Springbok QL. Site Fa11 samples the Copper Valley basalt: a localised basalt flow exposed only between two north–south trending faults in the north–east region of the Goboseb mountains (Fig. 2b).

3. Palaeomagnetic methods

The 737 cores and 149 hand samples were cut to standard 1 inch palaeomagnetic specimen size yielding a total of 1019 specimens (some cores yielded multiple specimens). Of these 1019 specimens, 893 were submitted to progressive demagnetisation. A combination of both stepwise thermal and alternating field (a.f.) demagnetisation techniques were used to test the stability of the natural remanent magnetism (NRM). Agico JR5A and Molspin magnetometers were used for measuring the magnetic remanence at Imperial College London and the University of Oxford palaeomagnetic laboratories with measurements conducted inside a dynamic Helmholtz cage (<30 nT, Imperial) and a shielded, field-free room (<500 nT, Oxford).

Thermal demagnetisation procedures were carried out using both ASC TD48 and MMTD1 palaeomagnetic ovens, with the capacity for 40 and 21 specimens respectively using up to 20 demagnetisation steps between 100 °C and 680 °C, reducing from 50 °C to 30/20 °C steps, with increasing temperature. Systematic reorientation of the specimens in the furnace was used to detect any laboratory induced magnetisations acquired through the heating/demagnetisation process. Alternating-field demagnetisation measure-

ments were carried out using a Molspin Tumbling a.f. demagnetiser up to 100 mT followed, where necessary, by a DTECH 2000 static demagnetiser up to 200 mT. The steps used were 0 mT, 5 mT, 10 mT, 15 mT, 20 mT, 30 mT etc. up to 100 mT. If required these steps were followed on the static instrument, by either 150 mT and 200 mT steps, or finer 120 mT, 140 mT etc. steps if the remaining remanence encompassed a large proportion of the total original NRM. On occasion, due to the presence of a mineral with high coercivity, a number of final heating steps were needed, starting at 500 °C and followed by further steps, at 540 °C and 580 °C, as required, to reduce the remaining magnetisation to below 5% of the original NRM. Of those specimens demagnetised using progressive thermal demagnetisation, 18 disintegrated on heating before full demagnetisation, leaving 875 fully demagnetised specimens.

The characteristic components of the NRM were determined by principal component analysis on linear portions of the orthogonal vector trajectories, with maximum angular deviations (MAD) <15° (Kirschvink, 1980). The majority of the fitted components had MAD values less than 5°. The primary and characteristic remanent magnetisation (ChRM), was taken to be the high-temperature/high-coercivity component of any multi-component remanence, with the lower temperature/coercivity component associated with either a (thermo) viscous overprint or a partial thermoremanent magnetisation acquired on subsequent re-heating by overlying lava flows. Where multiple specimens from a single core were analysed, the directions were averaged to produce a single core value. Site means were then calculated using Fisher (1953) statistics.

Rock magnetic measurements were made to help characterise the magnetic mineralogy and domain state of the samples. A Princeton Measurements vibrating sample magnetometer (VSM) was used to conduct room-temperature hysteresis curves (with an applied field of 500 mT and stepsize of 3 mT) and backfield curves (with 15–20 points). A furnace attachment was used to conduct high-temperature thermomagnetic curves for a select number of samples, these analyses were conducted in a Helium environment to minimise alteration by oxidation, with an applied field of 300 mT, a maximum temperature of 650 °C and temperature step-size of 1 °C.

4. Results

4.1. Magnetostratigraphy

Of the sampled 99 sites, 70 provided consistent palaeomagnetic directions. Samples from one site (Na3) all disintegrated on heating and a further 28 sites (202 specimens) yielded no consistent stable directions. Some of these specimens showed no linear components but the majority of failed sites showed internally scattered directions, comparatively high initial NRM intensities and were demagnetised at low field strengths (<40 mT). Their failure is therefore attributed to lightning induced isothermal remanent magnetisation (IRM) overprinting the primary remanence directions, and these sites are omitted from further discussion. The successful 70 sites, sampled by 673 specimens, provided consistent palaeomagnetic directions; 612 specimens, sampling 529 cores, were used to calculate the site means with the remaining 61 specimens, sampling 58 cores, being omitted from site mean calculations for the following reasons: (1) Cores providing directions far from the site mean that were broken during drilling and subsequently reoriented; (2) Cores from slightly different stratigraphic or lateral positions from the rest of the sampling site, providing directions distinct from the site mean; (3) Cores providing spurious directions while displaying soft demagnetisation behaviour and intensities double (or more) the other samples measured in that site, i.e., the remanence in these samples was likely a lightning induced isothermal remanence overprint; (4) Cores having no definable linear component of magneti-

sation. Post removal of these cores the data from these 70 sites exceed the Watson 1% significance values for grouping (Watson, 1956), with the exception of site Et11 which has too few samples for a valid application of the test; only four samples from this site survived demagnetisation without disintegrating, however, the directions were concordant.

With the exception of the omitted cores, most fully demagnetised specimens yielded a clear single identifiable linear component of magnetisation, with only a few sites (Na12, Na22, Na27 and Tg15) yielding two distinct linear components (defined by ≥4 measured points) (Dunlop, 1979; Zijderveld, 1967). The majority of specimens behaved in a very similar fashion during a.f. or thermal demagnetisation, with the removal of a minor viscous component in a.f. peak-fields of 15–20 mT or temperature treatments of 100–250 °C, followed by a linear ChRM component trending towards the origin on orthogonal demagnetisation plots. Representative plots from both thermal and a.f. demagnetisation are presented in Fig. 3. Given that both the Messum and Tafelkop sections are dipping, bedding corrections were carried out (supplementary Tables 1 and 2).

4.1.1. Etaka subgroup

The results of the palaeomagnetic analysis of the Grootberg and Bergsig sections are shown in Fig. 4 and the data presented in supplementary Table 1. The Grootberg section yielded directions from 27 sites, four of which record periods of reverse polarity. Only three sites failed to provide useful palaeomagnetic data (Na1, Na3 and Na26). The Bergsig section contains results from six individual sites, all showing normal polarity. Poor exposure prevented sampling of the lowermost Wêreldsend QL in this section.

The interpretation of Na12 and Na23 require further consideration. Na12 showed multicomponent remanence with consistent low temperature (≤350 °C) remanence and consistent (7/7 samples) high temperature remanence (reverse polarity). The observed multicomponent remanence is considered the result of overlying flow units causing thermal over-printing; the low temperature component displays a normal polarity direction consistent with the overlying flow (Na11) and consistent with a pTRM and the high temperature component is thus considered to reflect the primary remanence.

Na23, sampled the base of the ≈80 m thick Wêreldsend unit and displays single component reverse polarity remanence (8/8 samples). Sites lying stratigraphically above Na23, but still sampling the Wêreldsend, display normal polarity. We consider four possible explanations for this: (1) the flow is a single unit which underwent thermal overprinting, down to ≈50 m, however simple 'back of the envelope' calculations of thermal conduction suggest this is unlikely; (2) the recorded lower magnetisation is secondary and a result of self-reversal of the primary remanence, however self-reversal tests were conducted on a sample from Na23: first, it was a.f. demagnetised, second it was imparted with a laboratory TRM, and third it was subsequently a.f. demagnetised and there was no evidence for self-reversal, additionally as the site sampled the base of the Wêreldsend, the likelihood of self-reversal is reduced because of the association of self-reversal with partial oxidation, less likely at the base of flow units; (3) during cooling of the ≈80 m flow a reversal took place so only the basal chilled margin recorded the primary direction, however the expected overlying multicomponent remanence with high temperature components of reverse field and varying low field components is not seen; or (4) the thick unit is not a single flow and is in fact composed of multiple flows similar to sections at Terrace bay. We therefore conclude that the Wêreldsend QL consists of multiple flows, comparable to observations in coastal regions (Miller et al., 2008). Field logging shows observable differences and bulk rock
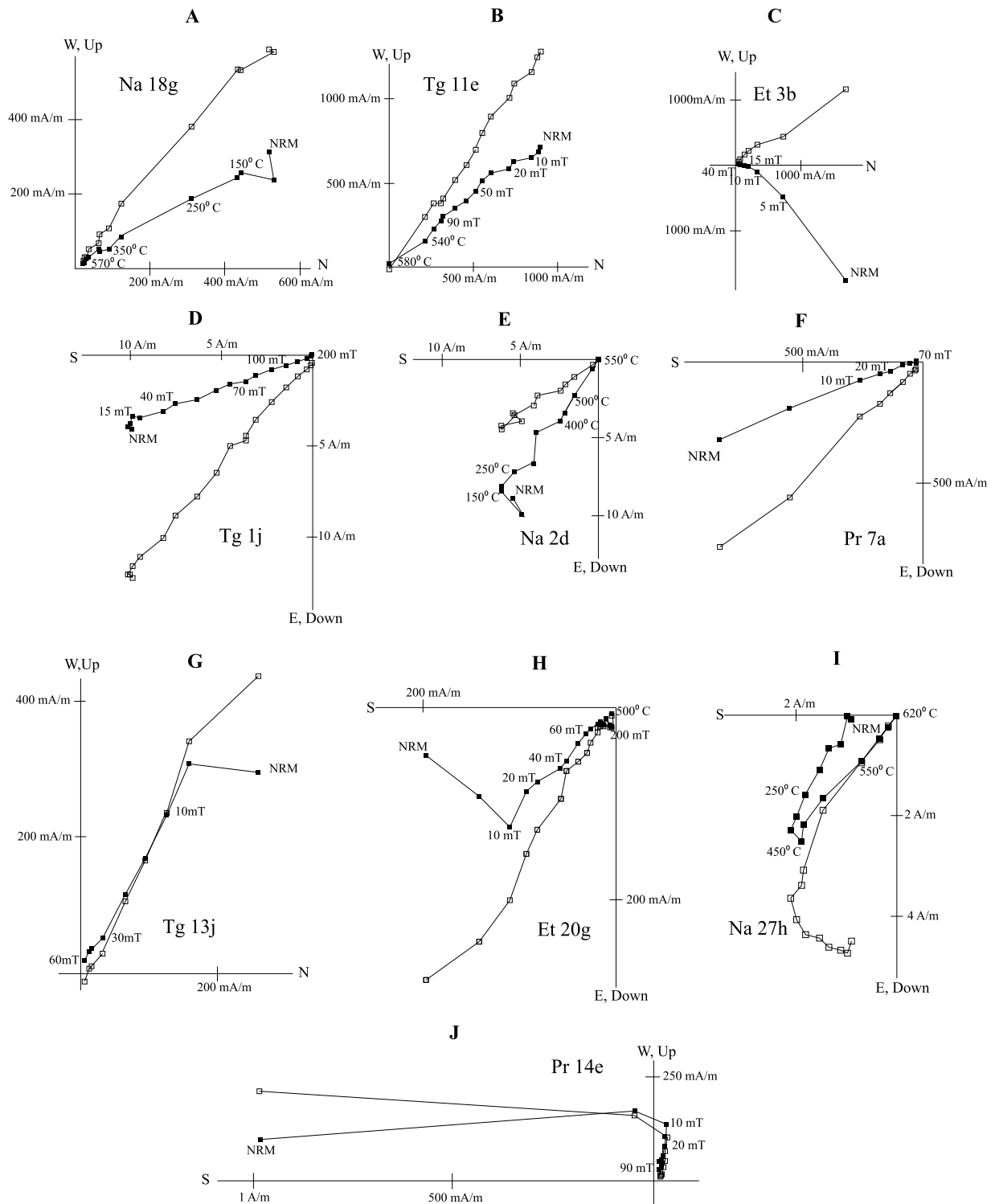
Fig. 3. Representative orthogonal plots illustrating samples recording periods of normal and reverse polarity by both demagnetisation methods. On orthogonal plots, solid (open) symbols represent horizontal (vertical) projections. A, B, G and J all illustrate samples recording normal polarity whereas D, E, F, H and I illustrate samples recording reverse polarity field states. The samples shown in A, E and I represent samples demagnetised using thermal demagnetisation whereas those samples shown in C, D, F, G and J represent samples demagnetised using alternating field. Those samples shown in B and H were demagnetised firstly by A.F. means however, some final thermal demagnetisation steps were required to fully demagnetise the samples. The sample shown in I is an example of multi-component remanence, with the higher temperature component taken as the ChRM. The sample in C is a sample suspected of representing a secondary isothermal remanence gained through a lightning strike. The sample demagnetises at lower a.f. peak field strengths and shows an anomalous direction. E, G, H and J all show examples of where a small component of viscous remanent magnetisation (VRM) is demagnetised prior to the linear ChRM. This component is too small to constitute a separate linear component being demagnetised by 15–20 mT/100–250 °C as discussed in the text.

geochemical analysis shows a progression in SiO_2 values through the unit which may suggest the unit is composed of three smaller flow units.

Taken as a complete section the grouped data from Grootberg and Bergsig passes the McFadden and McElhinny (1990) reversal test (Grade C: $\gamma_c = 14.26$, $\gamma_o = 11.26$).
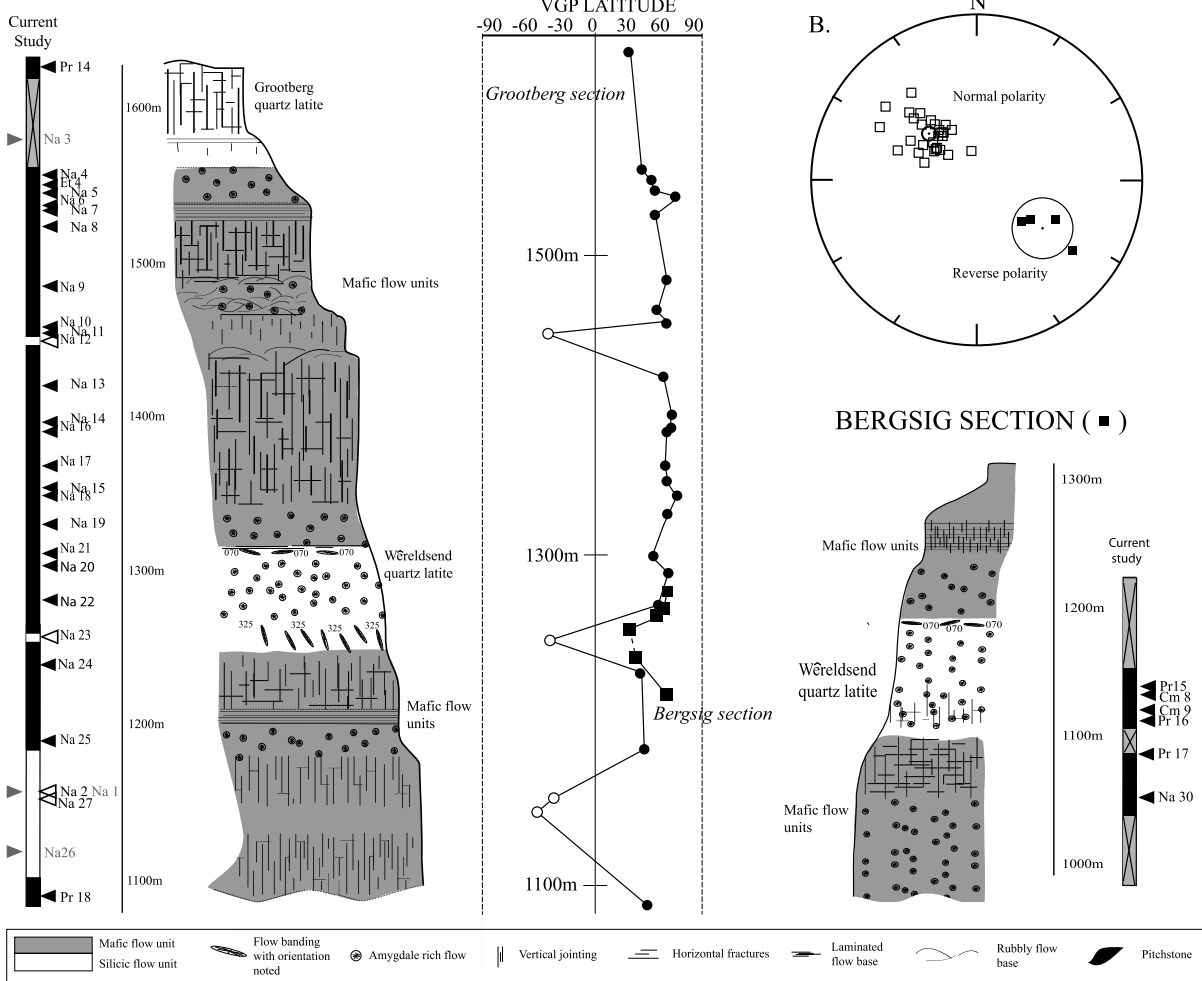
Fig. 4. Palaeomagnetic directions of the Grootberg section and the mini Bergsig section. Sites are presented along with their individual polarities (sites recording normal polarities are presented as black and reverse as white), the sites represented by grey symbols are those that failed to provide a consistent direction. A central plot of virtual geomagnetic pole (VGP) latitude with altitude is also presented (failed sites are not represented on this); both the Grootberg section and the Bergsig section are presented on a single VGP plot here, with the Bergsig absolute altitudes adjusted to their appropriate heights on the larger Grootberg section. The smaller inset B shows a stereonet including all of the site mean data. The circles of 95% confidence are shown for the reverse and normal site polarities respectively.

4.1.2. The Awahab subgroup

The results of the palaeomagnetic analysis of sites and sections sampling below the intra-Etendeka unconformity are shown in Fig. 5 and the data presented in supplementary Table 2. Although a higher proportion of the sites below the unconformity fail to yield consistent palaeomagnetic directions, a coherent magnetostratigraphy was still evident. Working from the base of stratigraphy upwards, in the Tafelkop section, 14/19 sites yielded consistent palaeomagnetic directions with seven sites recording reverse polarity. In the Messum section, 10/26 sites yielded consistent palaeomagnetic directions, five recording reverse polarity. The site sampling the Copper Valley basalt, which fits stratigraphically within the Messum section, recorded reverse polarity. A number of individual sites sampled the Springbok section in two localities. On the road to Torra bay 2/4 sites yielded consistent palaeomagnetic directions and both recorded normal polarity. On the Damaraland track the Springbok QL recorded a normal polarity whereas the underlying basalt recorded a reverse polarity (2/2 sites yielded consistent directions). In the Fonteine section, 8/11 sites yielded consistent directions. These sites spanned and sampled two individual QL units, a differentiation supported by intervening basalt units and by bulk rock geochemistry which places the units in different QL fields, according to the FeO versus TiO$_2$ separations

of Marsh et al. (2001). The upper Springbok QL recorded normal polarity (Et11), whereas the lower (Goboboseb II) QL recorded reverse polarity (Et8). Both of these observed polarities correlate with those obtained for these QL units at sites in other sections.

Taken as a complete section this data passes the McFadden and McElhinny (1990) reversal test (Grade C: $\gamma_c = 11.0$, $\gamma_o = 9.12$).

4.2. Rock magnetism

Room-temperature rock magnetic data was collected for representative samples from all sites providing useable palaeomagnetic directions in order to characterise the domain size and carrier of the magnetic remanence. For each of the lithologies sampled, hysteresis loops and backfield curves were conducted to characterise the size and so domain state of the magnetic remanence carriers. For a select number of sites, and all those displaying multi-component remanence, thermomagnetic analysis was conducted to characterise the mineralogy of the magnetic remanence carriers.

Hysteresis loops were generated for each site using rock chips obtained during the trimming of cores. From the hysteresis curves, combined with back-field curves, the following parameters were extracted: the coercive force (H_c), coercivity of remanence (H_{cr}),
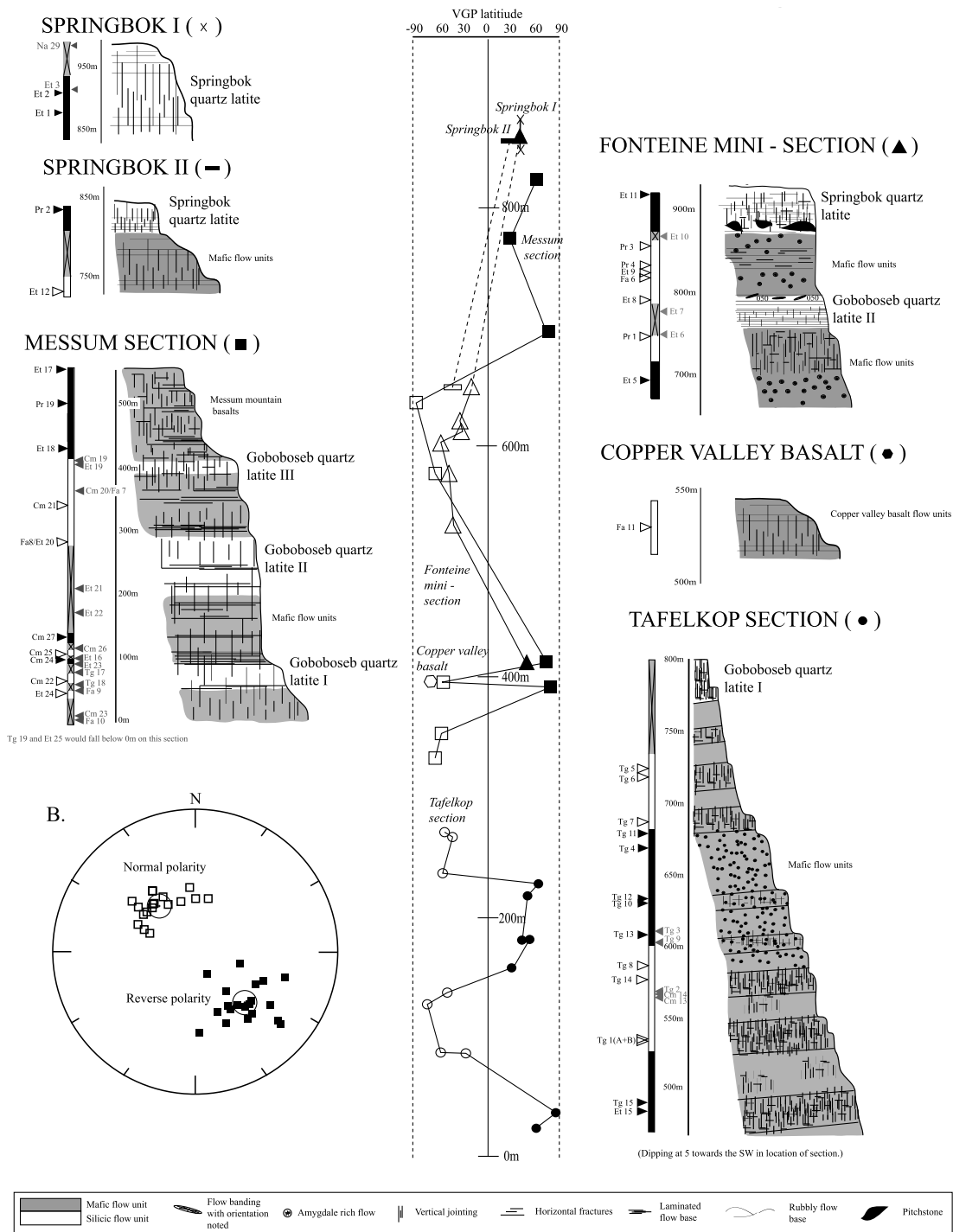
Fig. 5. Palaeomagnetic sections and individual sites sampling the lower Awahab subgroup. For the individual sections and sites altitudes given are taken straight from GPS readings. For the central composite magnetostratigraphy altitudes for the Messum and Tafelkop sections have been directly projected into a common vertical framework based on their dip and the radial distance of the site from the approximate centre of the Messum crater (21°25′0″ S, 14°12′55″ E). The Copper Valley basalt site has been placed in its correct stratigraphic position. In the case of the Springbok and Fonteine mini-sections vertical distances between sites have been 'stretched' in order to fit the composite section while respecting their correct relative stratigraphic positions. The smaller inset B shows a stereonet including all of the site mean data. The circles of 95% confidence are shown for the reverse and normal site polarities respectively.

saturation magnetisation (M_s) and remanent saturation (M_{rs}) (supplementary Table 3). The ratios of these parameters (M_{rs}/M_s versus H_{cr}/H_c) are plotted on a "Day plot" (Day et al., 1977) in Fig. 6 alongside several representative hysteresis loops. The majority (90%) of QL samples, alongside ≈99% of basaltic samples, fell within the pseudo-single domain (PSD) range according to Day et al. (1977), and this is typical for lavas dominated by magnetite and titanomagnetite. However, for QLs a slight trend towards

multi-domain (MD) state can be noted (i.e. Et8 and Cm8), and for basalts the opposite trend, towards single doman (SD) state, can be observed (i.e. Tg7). No evidence outside of this suggests the QLs to be any less capable of recording the remanence directions and although, when considering Et8 and Cm8, it is noted that the method by which remanence magnetisation is recorded in MD sized grains is not well understood, given the consistency of both within-site specimen directions and the directions recorded
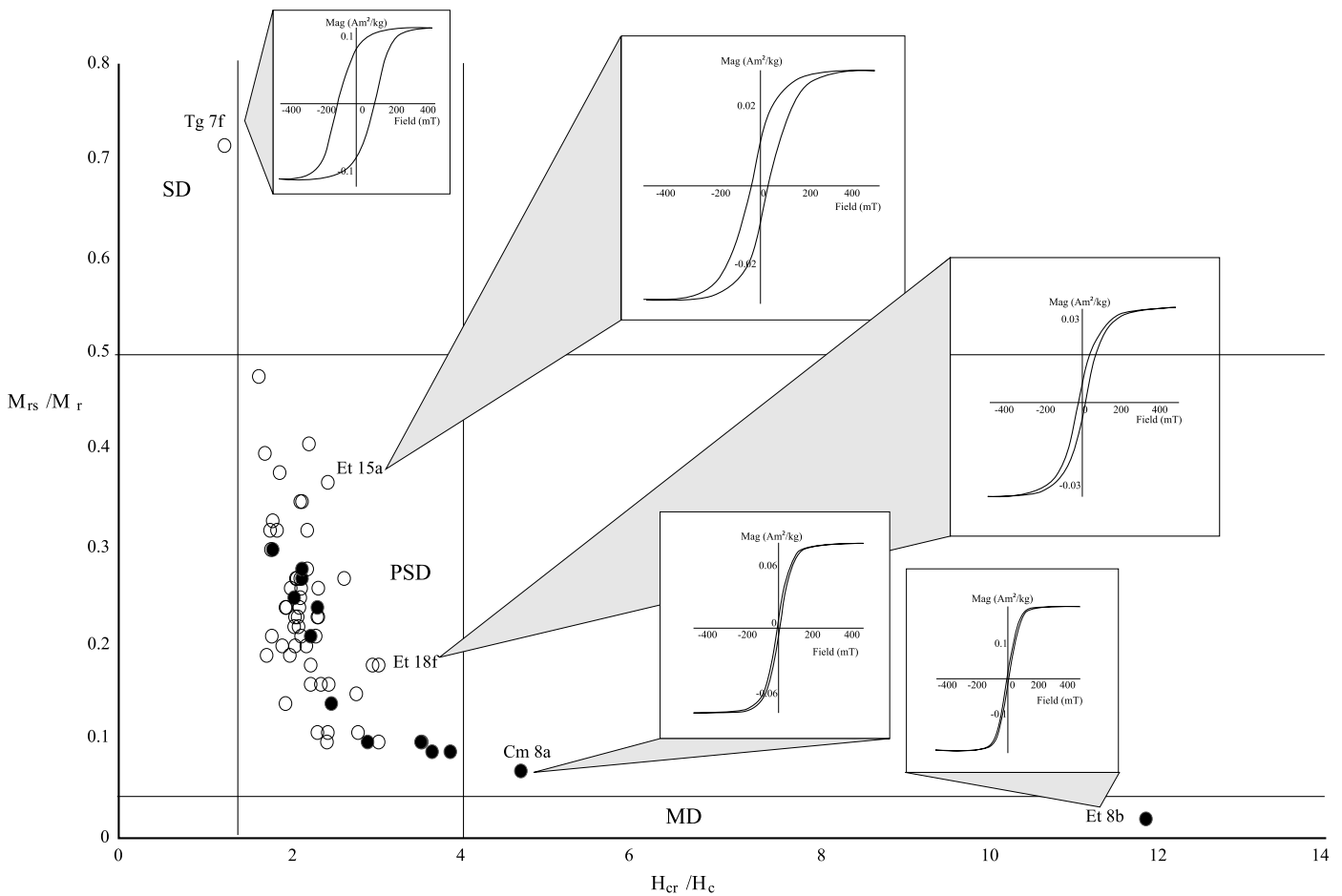
Fig. 6. A Day plot depicting the domain state of representative samples from all sites yielding stable palaeomagnetic directions. Hollow symbols represent basaltic sites and filled symbols represent quartz latite units. Insets are small hysteresis plots of the paramagnetically corrected data for individual samples illustrating examples of single domain, pseudo-single domain and multi-domain state specimens.
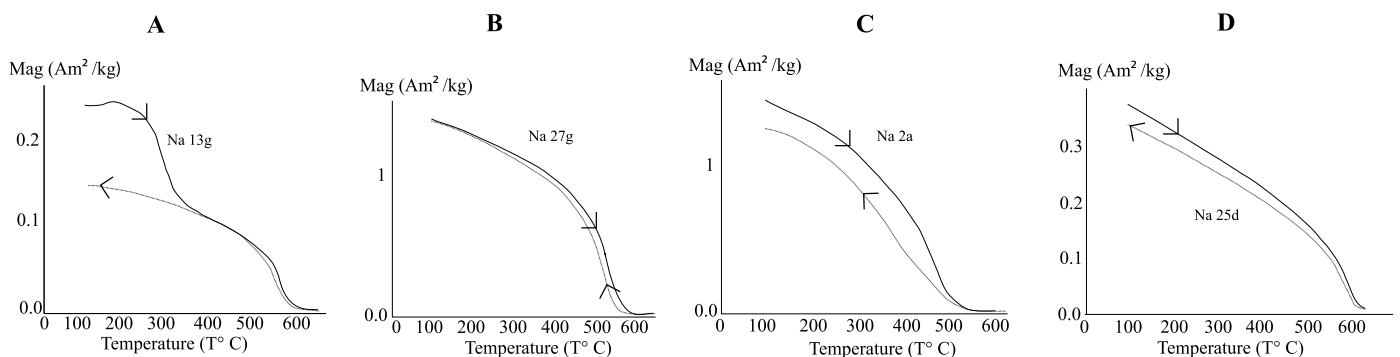

Fig. 7. Example thermomagnetic curves are presented. A, shows the curve of Na 13g (normal single component remanence). Multiple Curie temperatures can be noted on the heating curve but only one on the cooling curve, this suggests an inversion of the magnetic minerals recording the remanence occurred (see text for discussion). B, shows the curve of Na 27g (two-component remanence), this sample yields a single Curie temperature and a sharp intensity drop off during demagnetisation suggestive of a single Curie temperature in the pure magnetite region ($\approx 580\,°C$), the curves are also strongly reversible suggesting minimal alteration of the magnetic mineral (magnetite) is occurring on heating. C, shows the curve of Na 2a (single component reverse remanence), this sample is again showing a single Curie temperature this time in the titano-magnetite region (500–580 °C). The heating and cooling curves again appear reversible although some minor alteration seems to be occurring with the reversibility weaker than seen in Na 27g. D, shows the curve of Na 25d, it is reversible showing a single Curie temperature of 627 °C suggestive of titano-hematite being the main remanence carrying mineral.

by adjacent sites, these are still considered to be recording reliable directions.

The Curie temperatures (T_c) of selected site lithologies were determined by measuring thermomagnetic curves (Fig. 7). The second-derivative method (Tauxe, 1998), with running averages of 3, 5 or 7, was used, with T_c errors estimated to be at least $\pm 5\,°C$ (supplementary Table 3). Only a limited number of sites were cho-

sen for thermomagnetic analyses (22), with preference given to those showing multi-component remanence and those sites sampled in the earlier fieldwork seasons.

The thermomagnetic curves are divided into three characteristic type groups: (1) those with multiple, clearly defined T_cs (6/22) (e.g. Fig. 7a); (2) those with a single $T_c > 500\,°C$, but $\leq 580\,°C$ (13/22) (e.g. Fig. 7b/c); and (3) those with a single high $T_c >$

580 °C (3/22), (e.g. Fig. 7d). The majority fall within the second group indicating that titanomagnetites were the main remanence carrier with varying, but low, proportions of Ti^{4+} substitution (x) $(Fe_{(3-x)}Ti_xO_4)$. The titanium content ranged between $x = 0$ (T_cs close to pure magnetite at ≈ 580 °C), and $x = 0.16$, giving the lowest recorded T_c of just over 500 °C (Akimoto, 1962). The majority of sites falling within this group also displayed strongly reversible heating and cooling curves, indicative of little alteration during the heating process. The third group, with much higher T_cs, corresponds to those sites also noted as having a deep red–orange colouration. This is likely due to the presence of hematite or partially oxidised magnetite, which is in agreement with the higher T_cs recorded. These curves are predominantly reversible, with only minor differences between the heating and cooling curves. The first group can be split again into curves which show multiple well-defined T_cs on the heating curve but not on the cooling curve and are irreversible and those that show multiple T_cs on both heating and cooling. This type of behaviour indicates alteration and an inversion of magnetic minerals during the process of heating. The thermomagnetic curves for, for example, Na8j, Na13g and Na19i, are indicative of the inversion of (titano) maghemite to (titano) hematite, commonly found in surface weathered rocks (references as in Dunlop and Özdemir, 1997). The NRM directions recorded by these specimens showed no deflection during the temperatures spanning the inversion suggesting the remanence recorded was unaltered during this process and the site directions are thus considered robust.

5. Discussion

Of the sites sampled, 70/99 provided consistent magnetic directions with rock magnetic data identifying the main remanence carrier as predominantly titanomagnetite, as expected in volcanic rocks. There is a clear disparity between failure rates when comparing the sites sampling the Etaka and Awahab subgroups respectively. Only three sites sampling the Etaka subgroup failed to provide consistent remanence directions, whereas 26 failed from the Awahab subgroup. Of these 26, 18 were sites sampling the southern region (Messum/Tafelkop). This higher failure rate was attributed to two possible aspects of sample locality: (1) the rocks sampled in the Messum area provide the only 'real' topography, with the exception of Brandberg mountain to the east, and so may be more likely to have been struck by lightning than the sampled regions in the north, where there is a considerably higher density of topographic highs and (2) the northern sites sample mainly road cuts while the south samples mainly natural outcrop. This creates an apparently lower resolution magnetostratigraphy in the Messum region, which is a function of both this higher failure rate and an increase in scree cover.

Two new, high quality palaeopoles were calculated for South Africa from the both the Etaka and Awahab site VGPs, with values of, Plat: −47.2, Plong:84.2, A95:4.7 and Plat = −52.3, Plong:91.7, A95:6.1, respectively. These new poles are comparable with existing poles at 130 Ma for the global apparent polar wander path (APWP) in South African co-ordinates (Plat: −49.3°, Plong:80.9°, A95:2.8°) and the Gondwana APWP (Plat: −49.5, Plong:81.1, A95:4.4), from Torsvik et al. (2012) and in good agreement with the synthetic poles for South Africa at 130 Ma (Plat: −49.5, Plong:94.2, A95:7.4) and 135 Ma (Plat: −49.5, Plong:95.4, A95:5.6) from Besse and Courtillot (2002).

5.1. A new magnetostratigraphic record

We now consider these palaeomagnetic sections with respect to the proposed correlation in Marsh and Milner (2007) whereby the single reverse chron recorded within the Renne (1996b)

palaeomagnetic sections (Tafelberg (N–R–N), Awahab (N–R–N) and Tafelkop (N–R)) could be correlated. In support of this, correlations of basaltic flows between sections are presented, though no comparison of the magnetic directions for these flows was offered which, if sampling the same flow, should yield statistically indistinguishable values. Considering our more detailed palaeomagnetic sections (Fig. 8), we note the large number of previously unidentified reversals. Not only do these weaken the correlation of a single reverse polarity chron, but the majority of additional chrons are outside the suggested region for correlation. This means linking the sections would have only a minor effect on our estimate of the total duration of volcanism, given that only one newly noted reverse chron could correlate between sections.

Following this, we conclude that the Etaka and Awahab sections are not equivalent (with the notable difference in palaeopole values taken as support for this). A full composite Etendeka magnetostratigraphy was thus constructed, using all available unit polarities (including those of Renne et al., 1996b for the Nil Desperendum and the flow just below Goboboseb I Marsh et al., 2001) (Fig. 8b/c). This composite stratigraphy is based upon two assumptions: (1) no sites represent sills rather than flows and, (2) no additional chrons went unsampled. It suggests that Etendeka activity spanned a minimum of 16 polarity intervals, taking the minimum number to satisfy stratigraphic relationships below the unconformity.

5.2. Across the Atlantic

Marsh et al. (2001) present correlation of the Paraná and Etendeka QLs with four sections (BM, TA, PC and RA) in Milner et al. (1995) and Ernesto and Pacca (1988) presenting stratigraphy and corresponding palaeomagnetic sections. Although not possible to link complete palaeomagnetic sections across the Atlantic, it is possible to check for the expected polarity correlation between equivalent QLs. The unit equivalents in the Paraná, of the Grootberg, Springbok and Goboboseb, record the same polarity. The two Wêreldsend equivalents display normal polarity as seen in the upper Wêreldsend rather than the base reversal however, given the known lateral variation of this unit, it is unclear if the lower Wêreldsend is present or sampled in these Paraná sections. Although we cannot directly correlate the basalts we can observe common features between sections, e.g. in the TA section a reverse polarity interval is observed between the Grootberg and Springbok equivalents and a reversal occurs below the Springbok and Goboboseb equivalents in the BM and TA sections. In summary, although we cannot correlate the sequences fully, we can note that the Paraná sections seems to support, alongside the new Etendeka sections, a more complex magnetostratigraphy than was presented in Renne et al. (1996b), echoing the suggestion of >10 reversals suggested in Milner et al. (1995) for the Paraná magnetostratigraphy.

The Etendeka QLs are noted in places as showing evidence of hydrothermal alteration, we therefore consider the possibility the magnetisation measured is secondary. Numerous reversals are recorded within the sections, consequently rather than hydrothermal alteration affecting the whole lava pile post volcanism which should result in the lava pile recording a single polarity, this suggests instead that the remanence of only discrete layers would have to be affected with the QLs the most likely candidate for alteration. However, above, we note that, the unit equivalents in the Paraná, generally, record the same polarity and given the large lateral extent, and onset of separation at ≈125 Ma it seems unlikely that this is a later secondary magnetisation. We therefore consider the ChRM directions the result of primary magnetisation suggesting therefore that the Etendeka magnetostratigraphy is capable of
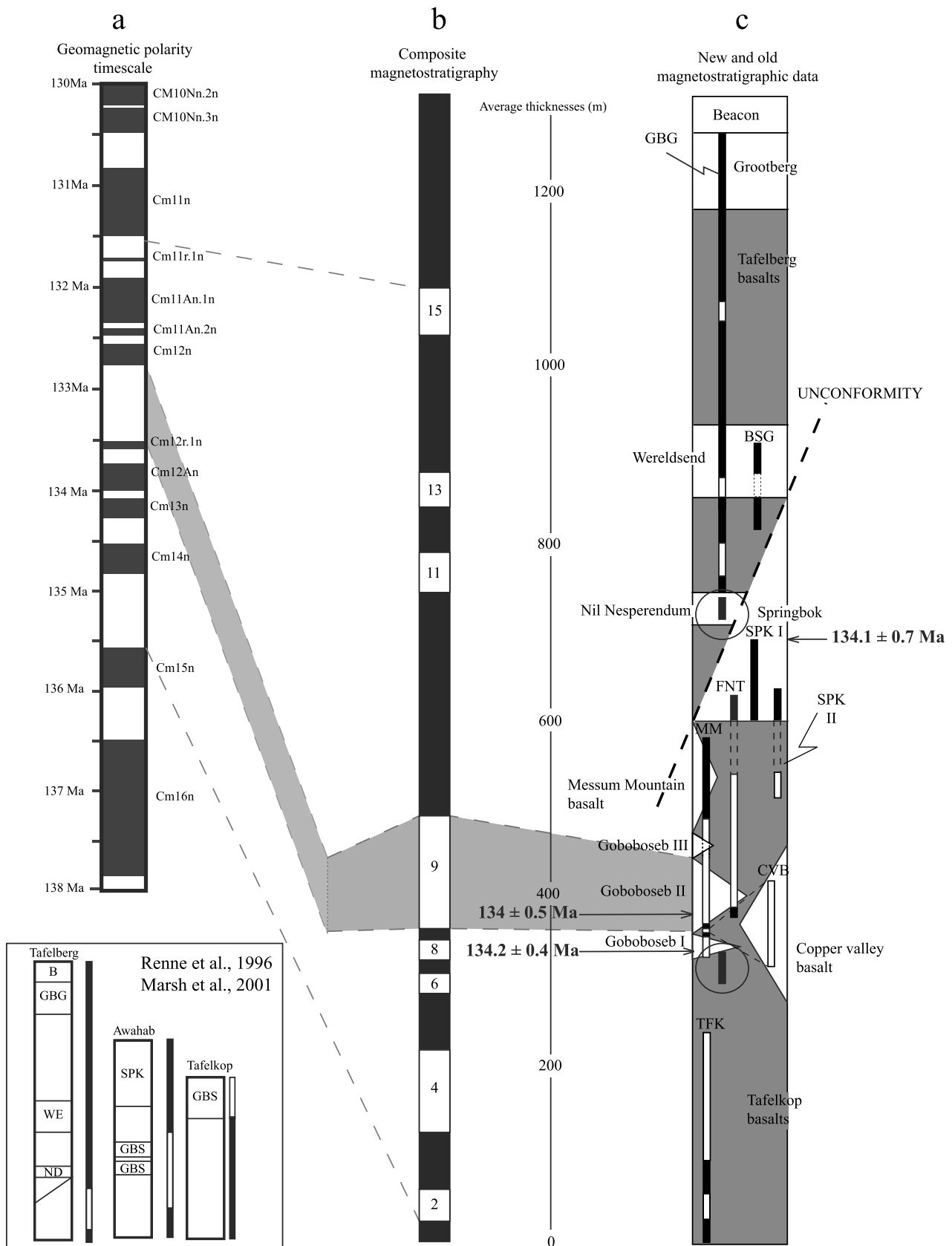
Fig. 8. A composite magnetostratigraphy established from this study and the polarities obtained in Renne et al. (1996a, 1996b) is shown in the centre. The small inset columns are simplified magnetostratigraphic columns showing the data of Renne et al. (1996a, 1996b). The right hand column illustrates the new magnetostratigraphy from this study with each individual section or sampling site marked (Grootberg – GBG, Tafelkop – TFK, Messum – MM, Springbok – SPK I and SPK II, Bergsig – BSG, Fonteine – FNT and Copper Valley basalt – CVB). The black circles mark the additional polarity constraints from Renne et al. (1996a, 1996b). A link to the geomagnetic polarity timescale (GPTS) is also postulated based upon the presented ^{40}Ar/^{39}Ar ages of Renne et al. (1996a, 1996b) adjusted to the new standard value (28.305 for the Fish canyon sanidine (FCs)) of Renne et al. (2010) and predominance of field behaviour.

providing a minimum duration of Paraná–Etendeka activity and perhaps a better indication of the style of this activity.

5.3. A Volcanic timescale for the Etendeka

We use the GPTS of Gee and Kent (2007) (Fig. 8a) to estimate the duration of volcanism assuming both the GPTS is accurate and that the reversal stratigraphy is correct. The Etaka stratigraphy is dominated by normal polarity punctuated by shorter periods of reverse polarity, whilst in contrast, the Awahab stratigraphy is characterised by a dominantly mixed polarity state. For the GPTS this apparent change in the predominance of normal and reversed polarity occurs at Chron 12(r/n). This finding broadly concurs with the constraints offered by the published $^{40}Ar/^{39}Ar$ ages of Renne et al. (1996b) (recalculated following Renne et al., 2010), we therefore link our magnetostratigraphy and GPTS using this central tie point (Fig. 8).

The duration of the intra-Etendeka unconformity is unknown. Given that the polarity does not change across the unconformity we suggest that it occurs within Chron 12n representing a substantial period of rapid erosion within this 250 kyr period. This is broadly consistent with both the published absolute ages spanning this interval that are within error (Renne et al., 1996b), and the conclusions of Wanke (2000) who argued the unconformity represents a period of very rapid erosion facilitated by the large area of fresh volcanic rocks undergoing rapid alteration and erosion. The estimated duration is therefore presented as a minimum (we assume the unconformity does not span two reversals). If the erosional period represented a long proportion of Cm12n, then the relative rates of extrusion before and after would appear elevated, however given that a large proportion of the accumulated thickness within Cm12n pertains to the three voluminous flows of the Springbok QLs, apart from high individual flow volumes, an overall spike in extrusion rates is not suggested.

Using the central tie point to the GPTS, the long period of normal polarity seen at the top of the province can be matched to Chron 11n and the normal polarity recorded at the base of the stratigraphy can be tentatively matched to Chron 15n. Assuming this correlation to be correct, volcanic activity lasted a minimum duration of 4 Myrs which is comparable to the ≈3 Myr estimate based upon existing absolute ages of Janasi et al. (2011) with this estimate tending to increase rather than decrease if this tie point is shifted.

5.4. Tempo of volcanism

Directional groups (DG)s have now been identified within several LIPs and many studies now use this method of analysis to establish the tempo of volcanic activity, with the identification of DGs suggesting pulsed magmatic activity (i.e. Chenet et al., 2008). For a set of adjacent flows to be part of a DG, the field they record has to be statistically identical i.e. the period of time elapsed between flows was not enough to record secular variation. We use the DG criteria of Chenet et al. (2008) to analyse our palaeomagnetic data.

Data from continuous portions of the upper and lower sections were analysed and found to show only two possible DGs, one consisting of only a pair of flows and one of four successive basaltic flows equating to only ≈50 m (<5%) of the total accumulated thickness (supplementary Table 4). When considered alongside Fig. 9, which presents accumulated Etendeka volcanic thickness against time, no evidence suggests the rate of volcanic activity was pulsed. Of course, accumulated thickness is not a direct measure of volume, given that it is a 2D measure of a 3D process, but nonetheless the first-order trend is suggestive of steady volcanism over time as is suggested by the distinct lack of large volume DGs.
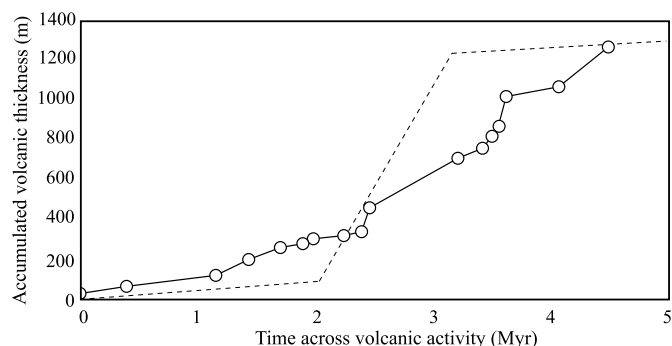

Fig. 9. A plot of accumulated thickness, as a proxy for volume, with respect to time (calculated from the suggested correlation with the GPTS in Fig. 8). The dashed line is a possible representation of the likely form of Deccan volcanic activity for comparison, with the majority of the province thickness/volume accumulated over a 1 Myr period of major activity, rather than the more constant activity suggested here for Etendeka volcanism.

Steady volcanism, would allow the recovery of Earth's ocean atmosphere system after individual flows, preventing the devastation instead possible following large pulses of voluminous magmatic activity.

Large igneous provinces are normally considered to have the bulk (75%) of their volume extruded within a 1–5 Myr period (Bryan and Ferrari, 2013) with estimates for many lying nearer 1 Myr (e.g. Courtillot and Fluteau, 2014). Estimates for the periods of major volcanic activity for the Deccan and Siberian LIPs stand at <1 Myr and <2 Myr respectively (Courtillot and Fluteau, 2014; Reichow et al., 2009). DG analysis, accompanied by Fig. 9, suggests that the rate of Paraná–Etendeka volcanism was fairly stable. This is in contrast to the rates suggested for the Deccan traps, where instead a high and episodic rate is suggested for a 1 Myr period with only minimal activity both before and after (Courtillot and Fluteau, 2014). Our estimate therefore places the duration of major volcanism in the Etendeka at the high end of these recent estimates, with no clear evidence for pulsed activity (Fig. 9). This prolonged timeframe suggests increased atmospheric and biological recovery time between individual eruptions. By allowing time for recovery between these flows and the high-flux release of volatiles, and by an overall reduction in volatile flux, it is suggested that large-scale atmospheric forcing and a global mass extinction may have been prevented. Coupling these extended periods of recovery with the lower volatile budgets recently proposed by Callegaro et al. (2014) and Marks et al. (2014) for Paraná–Etendeka volcanism, this may provide a suitable explanation for why this particular LIP seems not to have been associated with a mass extinction or major shift in Earth's climate.

6. Conclusions

We report a new extensive magnetostratigraphic study for the Etendeka portion of the Paraná–Etendeka LIP. Through high-resolution sampling, we have identified 16 polarity reversals. This new magnetostratigraphic data provides a minimum constraint on the total duration of volcanism of 4–5 Myrs, which is on the upper limit for the generally accepted time scale for LIPs, i.e., 1–5 Myrs. Compared to other LIPs of a similar volume, the relatively slow rate of Etendeka volcanic activity suggested by DG analysis, a corresponding decrease in the flux of volatiles coupled with a smaller initial volatile budget (Callegaro et al., 2014), and potentially increased recovery time between eruptions, may have prevented a global mass extinction. With the increasing precision on absolute ages being obtained for volcanic provinces (i.e. Blackburn et al., 2013), and the increasing use of DG analysis (i.e. Chenet et al., 2008), the ability for us to provide high resolution constraints for

LIPs is rapidly improving. This leaves no doubt that further studies of LIPs are needed which utilise all available techniques to establish increasingly detailed volcanic histories and provide a clear step towards developing an understanding of the relationships between these events and Earth's climate and biota.

Acknowledgements

Appendix A. Supplementary material

Supplementary material related to this article can be found online at http://dx.doi.org/10.1016/j.epsl.2015.01.009.

References

Akimoto, S., 1962. Magnetic properties of FeO–Fe$_2$O$_3$–TiO$_2$ system as a basis of rock magnetism. J. Phys. Soc. Jpn. 17, 706.

Besse, J., Courtillot, V., 2002. Apparent and true polar wander and the geometry of the geomagnetic field over the last 200 Myr. J. Geophys. Res., Solid Earth 107.

Black, B.A., Elkins-Tanton, L.T., Rowe, M.C., Peate, I.U., 2012. Magnitude and consequences of volatile release from the Siberian Traps. Earth Planet. Sci. Lett. 317, 363–373.

Blackburn, T.J., Olsen, P.E., Bowring, S.A., McLean, N.M., Kent, D.V., Puffer, J., McHone, G., Rasbury, E.T., Et-Touhami, M., 2013. Zircon U–Pb geochronology links the end-Triassic extinction with the Central Atlantic Magmatic Province. Science 340, 941–945.

Bryan, S.E., Ferrari, L., 2013. Large igneous provinces and silicic large igneous provinces: progress in our understanding over the last 25 years. Geol. Soc. Am. Bull. 125, 1053–1078.

Callegaro, S., Baker, D.R., De Min, A., Marzoli, A., Geraki, K., Bertrand, H., Viti, C., Nestola, F., 2014. Microanalyses link sulfur from large igneous provinces and Mesozoic mass extinctions. Geology 42, 895–898.

Chenet, A.L., Fluteau, F., Courtillot, V., Gérard, M., Subbarao, K., 2008. Determination of rapid Deccan eruptions across the Cretaceous–Tertiary boundary using paleomagnetic secular variation: results from a 1200-m-thick section in the Mahabaleshwar escarpment. J. Geophys. Res., Solid Earth 113.

Coffin, M.F., Eldholm, O., 1994. Large igneous provinces: crustal structure, dimensions, and external consequences. Rev. Geophys. 32, 1–36.

Courtillot, V., 1994. Mass extinctions in the last 300 million years: one impact and seven flood basalts. Isr. J. Earth-Sci. 43, 255–266.

Courtillot, V., Fluteau, F., 2014. A review of the embedded time scales of flood basalt volcanism with special emphasis on dramatically short magmatic pulses. In: Geological Society of America Special Papers, vol. 505, pp. 301–317.

Courtillot, V., Gallet, Y., Rocchia, R., Féraud, G., Robin, E., Hofmann, C., Bhandari, N., Ghevariya, Z., 2000. Cosmic markers, ^{40}Ar/^{39}Ar dating and paleomagnetism of the KT sections in the Anjar area of the Deccan large igneous province. Earth Planet. Sci. Lett. 182, 137–156.

Courtillot, V.E., Renne, P.R., 2003. On the ages of flood basalt events. C. R. Geosci. 335, 113–140.

Day, R., Fuller, M., Schmidt, V.A., 1977. Hysteresis properties of titanomagnetites: grain-size and compositional dependence. Phys. Earth Planet. Inter. 13, 260–267.

Dunlop, D., Özdemir, O., 1997. Rock Magnetism: Fundamentals and Frontiers. Cambridge University Press, Cambridge.

Dunlop, D.J., 1979. On the use of Zijderveld vector diagrams in multicomponent paleomagnetic studies. Phys. Earth Planet. Inter. 20, 12–24.

Erlank, A.J., Marsh, J.S., Duncan, A.R., Miller, R.M., Hawkesworth, C.J., Betton, P.J., Rex, D.C., 1984. Geochemistry and petrogenesis of the Etendeka volcanic rocks from South West Africa/Namibia. Spec. Publ., Geol. Soc. S. Afr. 13, 195–245.

Ernesto, M., Pacca, I., 1988. Paleomagnetism of the Paraná basin flood volcanics, southern Brazil. In: The Mesozoic Flood Volcanism of the Paraná Basin: Petrogenetic and Geophysical Aspects. LAG/USP, São Paulo, pp. 229–255.

Ernesto, M., Pacca, I., Hiodo, F., Nardy, A., 1990. Palaeomagnetism of the Mesozoic Serra Geral Formation, southern Brazil. Phys. Earth Planet. Inter. 64, 153–175.

Ernesto, M., Raposo, M., Marques, L., Renne, P., Diogo, L., De Min, A., 1999. Paleomagnetism, geochemistry and ^{40}Ar/^{39}Ar dating of the north-eastern Paraná magmatic province: tectonic implications. J. Geodyn. 28, 321–340.

Ewart, A., Milner, S., Armstrong, R., Dungan, A., 1998. Etendeka volcanism of the Goboboseb Mountains and Messum Igneous Complex, Namibia. Part I: geochemical evidence of early Cretaceous Tristan Plume melts and the role of crustal contamination in the Paraná–Etendeka CFB. J. Petrol. 39, 191–225.

Ewart, A., Milner, S., Duncan, A., Bailey, M., 2002. The Cretaceous Messum igneous complex, SW Etendeka, Namibia: reinterpretation in terms of a downsag-cauldron subsidence model. J. Volcanol. Geotherm. Res. 114, 251–273.

Fisher, R., 1953. Dispersion on a sphere. Proc. R. Soc. Lond. Ser. A, Math. Phys. Sci. 217, 295–305.

Gee, J.S., Kent, D.V., 2007. Source of Oceanic Magnetic Anomalies and the Geomagnetic Polarity Time Scale, Geomagnetism. Elsevier, Amsterdam, pp. 455–507.

Janasi, V.A., de Freitas, V.A., Heaman, L.H., 2011. The onset of flood basalt volcanism, Northern Paraná Basin, Brazil: a precise U–Pb baddeleyite/zircon age for a Chapecó-type dacite. Earth Planet. Sci. Lett. 302, 147–153.

Jay, A.E., Widdowson, M., 2008. Stratigraphy, structure and volcanology of the SE Deccan continental flood basalt province: implications for eruptive extent and volumes. J. Geol. Soc. 165, 177–188.

Jerram, D., Mountney, N., Holzförster, F., Stollhofen, H., 1999. Internal stratigraphic relationships in the Etendeka Group in the Huab Basin, NW Namibia: understanding the onset of flood volcanism. J. Geodyn. 28, 393–418.

Kirschvink, J.L., 1980. The least squares line and plane and the analysis of palaeomagnetic data. Geophys. J. R. Astron. Soc. 62, 699–718.

Marks, L., Keiding, J., Wenzel, T., Trumbull, R.B., Veksler, I., Wiedenbeck, M., Markl, G., 2014. F, Cl, and S concentrations in olivine-hosted melt inclusions from mafic dikes in NW Namibia and implications for the environmental impact of the Paraná–Etendeka Large Igneous Province. Earth Planet. Sci. Lett. 392, 39–49.

Marsh, J., Milner, S., 2007. Stratigraphic correlation of the Awahab and Tafelberg Formations, Etendeka Group, Namibia, and location of an eruptive site for flood basalt volcanism. J. Afr. Earth Sci. 48, 329–340.

Marsh, J.S., Ewart, A., Milner, S.C., Duncan, A.R., Miller, R.M., 2001. The Etendeka Igneous Province: magma types and their stratigraphic distribution with implications for the evolution of the Paraná–Etendeka flood basalt province. Bull. Volcanol. 62, 464–486.

McFadden, P., McElhinny, M., 1990. Classification of the reversal test in palaeomagnetism. Geophys. J. Int. 103, 725–729.

Miller, R.M., Becker, T., Geological Survey Namibia, 2008. 17. Early cretaceous Etendeka group. In: Becker, T. (Ed.), Neoproterozoic to Lower Palaeozoic. Illustrated ed. Ministry of Mines and Energy, Geological Survey (Namibia), Namibia.

Milner, S., Duncan, A., Ewart, A., 1992. Quartz latite rheoignimbrite flows of the Etendeka Formation, north-western Namibia. Bull. Volcanol. 54, 200–219.

Milner, S., Duncan, A., Ewart, A., Marsh, J., 1994. Promotion of the Etendeka formation to group status: a new integrated stratigraphy. Commun. Geol. Surv. Namib. 9, 5–11.

Milner, S., Duncan, A., Whittingham, A., Ewart, A., 1995. Trans-Atlantic correlation of eruptive sequences and individual silicic volcanic units within the Paraná–Etendeka igneous province. J. Volcanol. Geotherm. Res. 69, 137–157.

Peate, D.W., 1997. The Paraná–Etendeka Province. In: Mahoney, J.J., Coffin, M.F. (Eds.), Large Igneous Provinces: Continental, Oceanic, and Planetary Flood Volcanism. In: Geophysical Monograph Series, vol. 100. American Geophysical Union, Washington, DC, pp. 217–245.

Pinto, V.M., Hartmann, L.A., Santos, J.O.S., McNaughton, N.J., Wildner, W., 2011. Zircon U–Pb geochronology from the Paraná bimodal volcanic province support a brief eruptive cycle at ~135 Ma. Chem. Geol. 281, 93–102.

Raposo, M.I.B., Ernesto, M., Renne, P.R., 1998. Paleomagnetism and ^{40}Ar/^{39}Ar dating of the early Cretaceous Florianópolis dike swarm (Santa Catarina Island), southern Brazil. Phys. Earth Planet. Inter. 108, 275–290.

Reichow, M.K., Pringle, M., Al'Mukhamedov, A., Allen, M., Andreichev, V., Buslov, M., Davies, C., Fedoseev, G., Fitton, J., Inger, S., 2009. The timing and extent of the eruption of the Siberian Traps large igneous province: implications for the end-Permian environmental crisis. Earth Planet. Sci. Lett. 277, 9–20.

Renne, P.R., Ernesto, M., Pacca, I.G., Coe, R.S., Glen, J.M., Prévot, M., Perrin, M., 1992. The age of Paraná flood volcanism, rifting of Gondwanaland, and the Jurassic–Cretaceous boundary. Science 258, 975–979.

Renne, P.R., Deckart, K., Ernesto, M., Piccirillo, E.M., 1996a. Age of the Ponta Grossa dike swarm (Brazil), and implications to Paraná flood volcanism. Earth Planet. Sci. Lett. 144, 199–211.

Renne, P.R., Glen, J.M., Milner, S.C., Duncan, A.R., 1996b. Age of Etendeka flood volcanism and associated intrusions in southwestern Africa. Geology 24, 659–662.

Renne, P.R., Mundil, R., Balco, G., Min, K., Ludwig, K.R., 2010. Joint determination of ^{40}K decay constants and ^{40}Ar–^{40}K for the Fish Canyon sanidine standard, and improved accuracy for ^{40}Ar–^{39}Ar geochronology. Geochim. Cosmochim. Acta 74, 5349.

Self, S., Schmidt, A., Mather, T., 2014. Emplacement characteristics, time scales, and volcanic gas release rates of continental flood basalt eruptions on Earth. In: Geological Society of America Special Papers, vol. 505, pp. 319–337.

Tauxe, L., 1998. Rudiments of rock magnetism. In: Nolet, G. (Ed.), Paleomagnetic Principles and Practice. Springer, Netherlands.

Thiede, D.S., Vasconcelos, P.M., 2010. Paraná flood basalts: rapid extrusion hypothesis confirmed by new ^{40}Ar–^{39}Ar results. Geology 38, 747–750.

Torsvik, T.H., Van der Voo, R., Preeden, U., Mac Niocaill, C., Steinberger, B., Doubrovine, P.V., van Hinsbergen, D.J., Domeier, M., Gaina, C., Tohver, E., 2012. Phanerozoic polar wander, palaeogeography and dynamics. Earth-Sci. Rev. 114, 325–368.

Turner, S., Regelous, M., Kelley, S., Hawkesworth, C., Mantovani, M., 1994. Magmatism and continental break-up in the South Atlantic: high precision ^{40}Ar–^{39}Ar geochronology. Earth Planet. Sci. Lett. 121, 333–348.

Wanke, A., 2000. Karoo–Etendeka unconformities in NW Namibia and their tectonic implications. Julius-Maximilians University.

Watson, G.S., 1956. A test for randomness of directions. Geophys. J. Int. 7, 160–161.

Wigand, M., Schmitt, A.K., Trumbull, R.B., Villa, I.M., Emmermann, R., 2004. Short-lived magmatic activity in an anorogenic subvolcanic complex: ^{40}Ar/^{39}Ar and ion microprobe U–Pb zircon dating of the Erongo, Damaraland, Namibia. J. Volcanol. Geotherm. Res. 130, 285–305.

Wignall, P., 2001. Large igneous provinces and mass extinctions. Earth-Sci. Rev. 53, 1–33.

Wignall, P., 2005. The link between large igneous province eruptions and mass extinctions. Elements 1, 293–297.

Zijderveld, J.D.A., 1967. Methods in paleomagnetism. In: Collinson, D., Creer, K., Runcorn, S. (Eds.), Methods in Paleomagnetism. Elsevier, New York, pp. 254–268.